ELSEVIER

Chemical Engineering Journal 136 (2008) 331–336

Chemical Engineering Journal

www.elsevier.com/locate/cej

Photo-oxidation by singlet oxygen generated on nanoporous silicon in a LED-powered reactor

Alexei A. Lapkin [a,*], Veera M. Boddu [b,1], Gazi N. Aliev [a], Bernhard Goller [c], Sergej Polisski [c], Dmitry Kovalev [c]

[a] *Catalysis and Reaction Engineering Group, Department of Chemical Engineering, University of Bath, Bath BA2 7AY, UK*
[b] *U.S. Army Engineer Research and Development Center, Construction Engineering Research Laboratories, Champaign, IL 61826-9005, USA*
[c] *Department of Physics, University of Bath, Bath BA2 7AY, UK*

Received 14 January 2007; received in revised form 31 March 2007; accepted 3 April 2007

Abstract

An annular flow photochemical reactor illuminated by UV and green (524 nm) light emitting diodes (LEDs) was characterised by a chemical actinometer. Very high efficiency of absorption of photons, most likely promoted by the specific orientation of LED elements in the reactor, was calculated based on the measured actinometry results. Generation of singlet oxygen mediated by nanoporous silicon under illumination by Ar^+ laser, UV and green LEDs was demonstrated by indirect measurement of suppression of porous Si photoluminescence, and by direct measurements of singlet oxygen luminescence. The efficiency of reactor in singlet oxygen mediated reactions was tested using reaction of decomposition of diphenylbenzofuran. Estimated quantum yield of chemical reaction is about 34%.

Keywords: Nanoporous silicon; Singlet oxygen; Photochemistry; Continuous processes

1. Introduction

Activation of chemical bonds by light is one of the less-exploited strands of green chemical technologies. It offers selective transformations of functional groups in complex molecules and has proven applications in photo destruction of pollutants. Only a small number of photochemical or photocatalytic processes have been commercialised on a large scale. This is mainly due to (i) inefficiency of light delivery, *i.e.*, light scattering by solvents and particulates, (ii) poor scaleability due to high energy consumption, difficulties with light absorption, hydrodynamics and mass transfer limitations on a large scale, and finally (iii) high cost of delivery of molar quantities of photons [1]. These problems are common to major areas of photomediated processes, namely destruction of airborne pollutants, pathogens, removal of organic or metal salts water contaminants, and synthetic photochemical processes.

A number of innovative approaches to photochemical processes, which address these main problems, have been proposed. These approaches include: heterogenising photocatalysts, use of new types of light sources and transition to microreactors. Heterogenising photocatalysts avoids the problems of light scattering on nanosized catalyst particles, enables more efficient delivery of light per specific surface area ($m^2\ m^{-3}$) of a reactor and, more significantly, avoids expensive downstream catalyst separation, which may account for the majority of the process running costs. A number of heterogenisation approaches have been suggested. These included deposition of photocatalysts on tubular reactor walls [2], membranes [3] or other supports such as monoliths [4], structural packing [5], or directly onto light sources such as side scattering optical fibres [6,7] or packaged light emitting diodes [8].

The use of narrow monolith channels [9] or microreactors [10–14] improves mass transfer, especially in the liquid phase applications, and considerably increases the specific illuminated area. Separation of total flow into narrow channels also simplifies scale-up, which in this case is achieved by numbering up of parallel tubes. This was recently demonstrated using a simplified model of a continuous photoreactor [15].

* Corresponding author. Tel.: +44 1225 383360; fax: +44 1225 385713.
E-mail address: A.Lapkin@bath.ac.uk (A.A. Lapkin).
[1] On sabbatical at the University of Bath.

1385-8947/$ – see front matter © 2007 Elsevier B.V. All rights reserved.
doi:10.1016/j.cej.2007.04.013

An area of increasing interest in photochemical processes is the use of light emitting diodes (LEDs) as light sources instead of conventional mercury, deuterium or xenon lamps [8,10,16,17]. With the rapidly decreasing cost of LEDs due to developments in novel materials and mass marketing opportunities of solid state lighting, application of high-power light emitting diodes and lasers in chemical engineering becomes economically viable. Two potentially very significant applications of LEDs in process chemistry stem from their relatively narrow range of emission wavelengths. This should allow selective activation of specific bonds [18] and new control applications, *i.e.* real time process optimisation aided by fast in situ chemical optical sensing, and self-regulating processes. Although there are already several reports and patents in the public domain on the application of LEDs in photochemistry/photocatalysis, there is no detailed data on their power conversion efficiency. It is addressed in the present paper.

Recently, a very efficient generation of singlet oxygen ($^1O_2$) due to energy transfer from excitons photoexcited in a wide visible range and confined in silicon nanocrystals forming porous Si (PSi) layers was reported [19–21]. This system has a highly developed surface accessible to oxygen molecules, size-tuneable energy of electronic excitations (excitons) and a very long radiative lifetime. These factors are favourable for achieving a high efficiency of the energy transfer from photoexcited excitons to oxygen molecules. The quantum efficiency of Si nanocrystals as sensitizer of singlet oxygen at room temperature is *ca*. 0.9 [19], which is higher than that of Rose Bengal (0.86) [1], the best known singlet oxygen sensitizer until now. This discovery may lead to a rapid development of efficient processes utilising singlet oxygen, for which a very large number of reactions have already been studied [22]. One of the first reported reactions of singlet oxygen generated by photoexcited nanocrystalline silicon is degradation of 1,3-diphenylisobenzofuran (DPBF) [21,23]. The latter is known to be highly reactive with singlet oxygen exclusively via chemical quenching [24]. Earlier reports on the degradation of DPBF by singlet oxygen generated by photoexcited PSi used very expensive silicon materials prepared by electrochemical etching of (1 0 0) oriented Si wafers. Current study reports the development of a practical semi-continuous laboratory scale reactor with green and UV light emitting diodes as light sources, and using nanocrystalline silicon obtained by a cheap and readily scaleable wet chemical etching method from metallurgical grade Si powder. This paper uses the model reaction of degradation of 1,3-diphenylisobenzofuran and liquid ferrioxalate actinometer to characterise the efficiency of reactor illumination and proof-of-concept calculations on the feasibility of photochemical reactions in the system with 524 nm LEDs and porous silicon.

2. Experimental

Green and UV LEDs were purchased from Farnell (USA). Green LEDs were assembled into four strips of 24 diodes each. Each strip could be controlled separately. The UV LEDs were assembled into a strip of 50 surface mounted chips. The green LED strips were mounted onto a dark plastic case, providing a 15 cm long illumination zone, surrounding a thermostated glass annular flow reactor with a 1.5 mm thickness of annular space and 9.5 ml total reaction volume. In the case of UV LEDs, a single strip was placed inside the quartz reactor. LEDs were powered using a 60 V power supply via Supertex CL2 LED drivers. The experimental set-up is shown schematically in Fig. 1, which also gives details of the design of the glass and quartz flow reactors. Gases (N_2, O_2) flow rates were controlled by Bronkhorst mass flow controllers. A gear pump was used for the liquid flow. Liquid and gas were mixed in a *t*-piece at the inlet into the reactor and directed upwards, establishing slug annular flow. The temperature of the glass reactor was maintained by circulating thermostated water through the inner reactor tube, whereas in the case of the quartz reactor, the outer jacket was used for heat transfer. A solution of reactants and porous silicon particles in the liquid reservoir was continuously stirred during the reaction. The gas vent line from the reservoir (gas-liquid separator) was equipped with a heat exchanger, kept at about 5 °C to reduce solvent loss.

Porous Si (PSi) powder was prepared by stain etching of metallurgical grade polycrystalline Si powder, having a mean particle size about 4 μm. The aluminum-doped Si powder was immersed in an aqueous hydrofluoric acid solution, then HNO_3

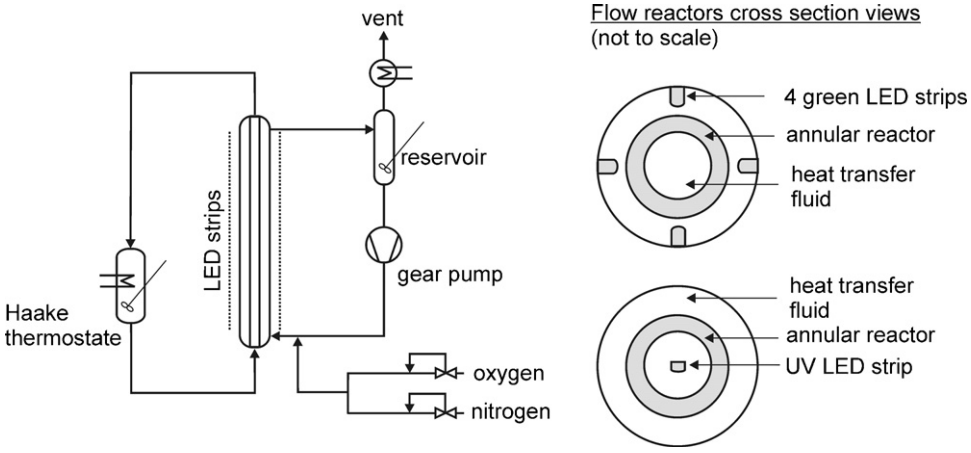

Fig. 1. Schematic diagram of photochemical flow reactor utilising LEDs for illumination.

was added gradually until the ratio of used chemicals was *ca.* 20:4:1 of H_2O:HF:HNO_3. Depending on the desired size distribution of Si nanocrystals assemblies, the etching process was terminated when the initially metallic colour of the powder had changed to brown-yellow, and an efficient redorange photoluminescence was seen under illumination by ultraviolet (UV) light. This photoluminescence is due to radiative recombination of photoexcited electron–hole pairs (excitons) geometrically confined in Si particles. This ensures that the size of formed Si nanocrystals, assembling porous grains, is in the nanometre range [22]. To obtain a highly reactive hydrogen-terminated PSi surface all the HNO_3 needs to be consumed from the etching solution, which is achieved by having an excess of HF. The obtained PSi powder was hydrophobic and was collected and dried in ambient air or in vacuum at around 40–70 °C. This yielded a mean pore size distribution, as estimated by the Barrett–Joyner–Halenda (BJH) method, of approximately 3–5 nm.

Actinometry was measured following the Hatchard–Parker procedure [25]. The ferrioxalate actinometer is sensitive between 577 and 253 nm and the quantum yield of Fe^{2+} at green light irradiation (measured peak intensity at 524 nm), estimated from the original Hatchard and Parker data by interpolation, is *ca.* $\Theta_{Fe^{2+}} = 0.58$. The intensity of two (48 LEDs) and four (96 LEDs) green LED strips was measured under flow conditions (liquid circulation around the reactor).

Generation of singlet oxygen in the continuous photochemical reactor was detected directly by photoluminescence (PL) from singlet oxygen and indirectly by quenching of the PSi luminescence. PSi (0.2 wt.%) with a mean particle size of *ca.* 4 μm and specific surface area of *ca.* 200 $m^2\,g^{-1}$ solution in CCl_4 was used. An Ar^+ laser (488 nm, intensity about 1 $W\,cm^{-2}$), four green LED strips (524 nm, intensity about 10 $mW\,cm^{-2}$) illuminating a glass reactor, one UV-LED strip inside a quartz reactor and a 3-chip UV LED element illuminating the quartz reactor were used to excite PSi particles. PL spectra in the visible range were measured using a spectrometer equipped with a gated charge-coupled device. All spectra were normalised and corrected to the sensitivity of the detection system.

Photo-degradation of DPBF, obtained from Fisher Scientific, was measured by monitoring the intensity of absorbance at 430 nm. Samples were filtered prior to absorption measurements to avoid the influence of PSi particles. One millimolar solution of DPBF in CH_2Cl_2 was pumped with 40 ml min^{-1} flow rate. Oxygen flow rate was 30 and 50 ml (STP) min^{-1}. Reactor temperature was kept at 20 °C in all reactions.

3. Results and discussion

3.1. Efficiency of reactor illumination using LEDs

The power output of a single LED was measured by a standard power meter, and is *ca.* 2.0–2.5 mW. This value is in agreement with the manufacturer's power specification of 0.9–2.68 mW, depending on the feed current. In the actual set up, 96 LEDs 12 drivers were used to ensure current stability, with total maximum power consumption 8.34 W. Hence, the efficiency of power to light conversion is about 2.3–2.9%. Without drivers, which were included to ensure stability of feed current, the power conversion increases to 3.5%. These values are still low to compete with conventional light sources, which routinely deliver about 40% power-to-light conversion efficiency.

The efficiency of electrical input power to absorbed photons conversion was estimated on the basis of actinometry measurements. Maximum intensity of the green LEDs was measured to be around 524 nm, see inset in Fig. 2. This corresponds to the quantum efficiency of ferrioxalate actinometer of 0.58 [25]. The absorbance of actinometer with the specific concentration used in this study is, however, quite low *ca.* 5.4×10^{-4} based on the data from [25]. Therefore, the actinometer will allow a reasonably accurate measurement of absorbed photons, but a less accurate measurement of the intensity of the LED light source. Measurements were performed in the system with four independently controlled strips of 24 LEDs located at 90° around a glass reactor, see Fig. 1.

The absorbance of actinometer following illumination by 48 and 96 LEDs is shown in Fig. 2a. The number of absorbed photons per second can be calculated from Eqs. (1) and (2). Eq. (1) gives the number of absorbed photons per unit time measured by UV–vis analysis of the fixed actinometer solutions [26], whereas Eq. (2) accounts for the volume of solution being illuminated at any moment in time in the continuous re-circulation experiment [27]:

$$n_{a,measured} = \frac{1}{\Theta_\lambda t} \frac{6.023 \times 10^{20} V_2 V_3 \log(I_0/I)}{V_1 l \varepsilon} \quad (1)$$

where V_1 is the volume of irradiated actinometer solution (ml) taken as total volume of the circulating liquid, assumed to be approximately equal to the tank volume V_T, V_2 the volume of actinometer aliquot, V_3 the final volume of sample after dilution, $\log(I_0/I)$ the measured optical density, ε the molar extinction coefficient of solution obtained from calibration ($dm^3\,mol^{-1}\,cm^{-1}$), and Θ_λ is the quantum yield of actinometer at given excitation wavelength, l is the cuvette path length (cm)

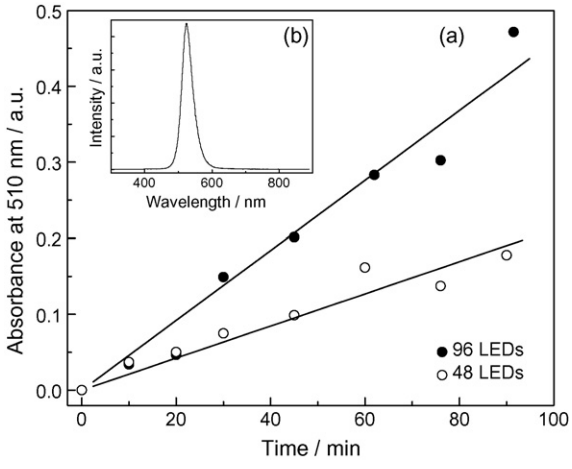

Fig. 2. Absorbance of ferrioxalate actinometer with two and four green LED strips; (b) emission spectrum of green LEDs.

and t is the irradiation time (s):

$$n_a = \left(\frac{V_R + V_T}{V_R}\right) n_{a,measured} \quad (2)$$

where V_R is the volume of reactor, *i.e.*, the illuminated annular space in the glass reactor in this specific case, and V_T is the volume of liquid tank or reservoir. This equation is valid in the approximation of negligible volume of connecting tubes, which is satisfied in this work.

Thus, for 48 and 96 LED elements the number of absorbed photons was calculated as 4.1×10^{-7} and 8.3×10^{-7} E s^{-1}, respectively, or 94 and 190 mW in power units. The value of absorbed photons corresponds well with the total light power provided by the LEDs, which is estimated to be between 190 and 240 mW for 96 elements on the basis of power output of a single element. Therefore, it appears that the circular design of the light source allows highly efficient utilisation of light, despite low absorbance of solution at 524 nm and short direct pathlength of about 1.5 mm. This is likely to be due to the specific arrangement of LED elements, which promoted reflection and concentration of light within the central reactor area. The overall efficiency of input electrical power to absorbed photons with 96 green LED elements is about 2.3%. Furthermore, the green light source is well suited to the absorbance of PSi micropowder. The absorption coefficient of PSi layers measured at 525 nm is ~500 cm^{-1} [28] and, therefore, the entire core of porosified Si grains is excited uniformly.

Although the power conversion efficiency of about 2.3% is rather low, there are several significant advantages of light emitting diodes in photochemical applications. The narrow emission spectra ensure that all generated light is in the region of interest and there are no losses due to filters. The small size of LEDs surface allows concentrating light sources in a very small space, as well as mixing several wavelengths into a spectrally modulated light source. LEDs could be assembled into different shapes of illuminating surfaces. Finally, the long lifetime and low hazard in comparison with, *e.g.* mercury lamps make LEDs considerably easier to use in the laboratory or industrial environment. As it is shown below, the reactor with 96 green LED elements was sufficient to generate and utilise singlet oxygen using PSi as a sensitizer.

3.2. Detection of $^1O_2$ in the flow photochemical reactor

As it was shown earlier [20], generation of singlet oxygen is efficiently mediated by photoexcited Si nanocrystals assembling PSi. To demonstrate the efficient energy transfer from Si nanocrystals to O_2, we compared PL spectra of H-terminated PSi powder in nitrogen and oxygen saturated CCl_4, *i.e.* in deoxygenated and oxygenated media (Fig. 3). CCl_4 was used due to the relatively long lifetime of the singlet oxygen in this solvent [29], which simplifies its detection using spectroscopic techniques. In the presence of dissolved oxygen, a strong and energy-dependent reduction of the silicon PL intensity due to energy transfer from Si nanocrystals to oxygen molecules is observed. In order to eliminate the effects of the spectral shape caused by the size distribution of the Si nanocrystals, we derive

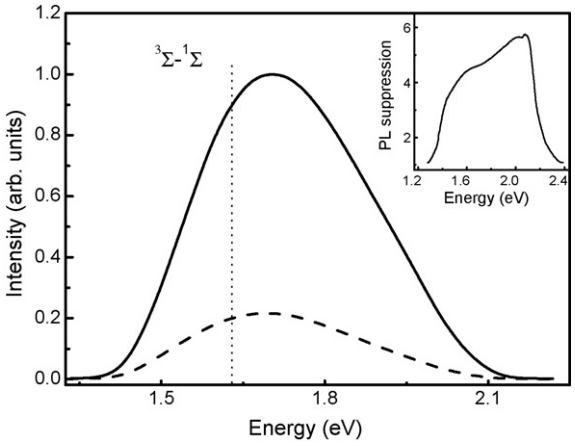

Fig. 3. PL spectra measured in de-oxygenated CCl_4 (solid line) and in oxygenated CCl_4 (dashed line). Inset: spectral dependence of the PL suppression level for oxygen-saturated CCl_4. $T = 300$ K, $E_{ex} = 2.54$ eV. Energy of the $^3\Sigma$–$^1\Sigma$ transition of O_2 is indicated by a dotted line.

the PL suppression level as the ratio of the PL intensity measured with and without O_2.

The energy-dependent coupling strength of excitons confined in Si nanocrystals and O_2 is seen in the PL suppression level (inset of Fig. 3). The PL suppression level at the energy of the singlet–triplet transition ($^3\Sigma$–$^1\Sigma$) of O_2 at 1.63 eV is around 4.5. The strong PL quenching in the presence of oxygen is due to a nonradiative energy transfer from the exciton to O_2, resulting in the activation of a singlet oxygen state. This implies that more than 80% of the photoexcited excitons transfer their energies to O_2.

Based on the measured efficiency of conversion of excitons into singlet oxygen it is possible to estimate the generation rate of singlet O_2 in the pores of PSi. For this calculation, we have measured absorption coefficient at 488 nm of a solution containing 0.2 wt.% PSi in a 1 cm thick cuvette, which was found to be 3.5 cm^{-1}. Using this value, the rate of generation of singlet oxygen in the oxygen saturated solution at ambient pressure and at excitation intensity of Ar^+ laser (488 nm) of 1 W cm^{-2} is about 4.6×10^{-4} mol (singlet oxygen) dm^{-3} s^{-1} (this value assumes 80% efficiency of conversion of exciton to singlet oxygen and 5% efficiency of conversion of photons into excitons). In the case of the green LED light source, we can use the actual value of absorbed photons, measured by actinometry (*ca.* 190 mW). Therefore, the rate of generation of singlet oxygen within the annular space of the photochemical reactor in this case is about 3.5×10^{-6} mol dm^{-3} s^{-1}. This value can later be used to estimate the quantum yield of a chemical reaction.

Suppression of PSi photoluminescence is an indirect method of proving the generation of singlet oxygen. The excited $^1\Sigma$ state of oxygen rapidly relaxes mainly nonradiatively into the $^1\Delta$ state. Therefore, the only possible direct evidence of singlet oxygen generation is the detection of near infrared (NIR) luminescence band caused by $^1\Delta$–$^3\Sigma$ transition. We measured NIR spectra using a single monochromator equipped with a liquid N_2 cooled InGaAs near infrared diode array. Fig. 4 shows the NIR luminescence band of singlet oxygen mediated by PSi powder excited by different light sources, having different excitation

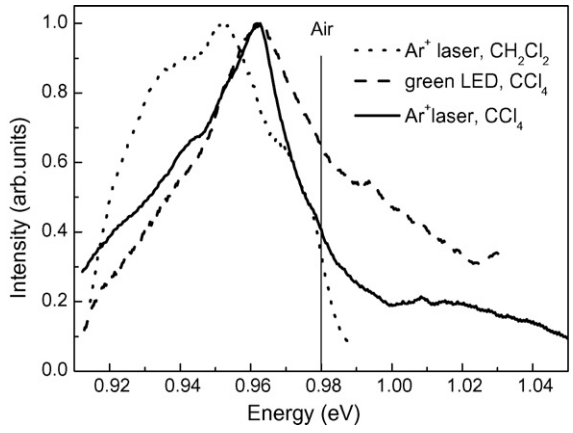

Fig. 4. Emission lines of singlet oxygen, generated by photoexcited porous silicon—Ar^+ laser: $E_{ex} = 2.54$ eV and green LEDs. The $^1\Delta$–$^3\Sigma$ transition of molecular oxygen in gaseous phase is indicated by vertical line.

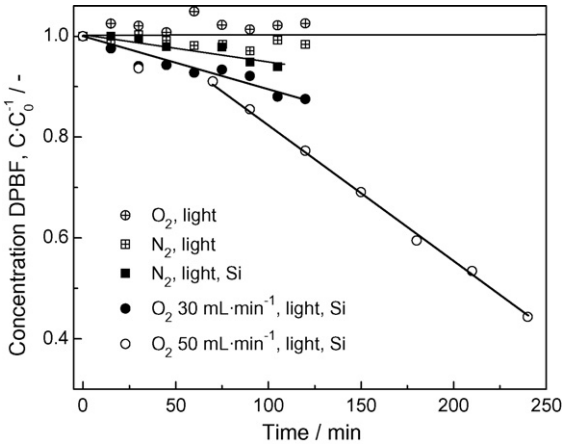

Fig. 5. Photodegradation of 1,3-diphenylisobenzofuran (DPBF) at ambient temperature under green light LED illumination. Experimental conditions are indicated in the figure. Gas flow rate is 30 ml min^{-1}, unless otherwise specified. Reaction temperature 20 °C. Liquid flow rate 40 ml min^{-1}.

energies and intensities. These measurements were performed in the quartz and glass reactors, shown schematically in Fig. 1. Based on the literature data on the lifetime of singlet oxygen in CCl_4 (2.6×10^{-2} s [30]) and the rate of generation estimated above, the steady state concentration of singlet oxygen was about 2×10^{-2} mol dm^{-3} when Ar^+ laser has been used. These results illustrate that photoexcited PSi is a very efficient generator of singlet oxygen, regardless of the used excitation energies (in Fig. 4 only results for Ar^+ laser and green LEDs are demonstrated but identical results were obtained for UV LEDs) and their powers.

Singlet oxygen luminescence was also detected in 1,2-dichloroethane, with the position of $^1\Delta$–$^3\Sigma$ transition slightly shifted relative to that in CCl_4 and air, see Fig. 4. Because of considerably faster nonradiative energy relaxation of singlet oxygen in the presence of C–H bonds having high vibronic energy, the lifetime of singlet oxygen is about three orders of magnitude shorter, 6.3×10^{-5} s [30], compared with CCl_4. This results also in the very low steady state concentration of singlet oxygen, about 4–5 $\times 10^{-5}$ mol dm^{-3}. Despite this low concentration the generation of singlet oxygen can still be detected via the direct optical measurement.

3.3. Photodegradation of diphenylisobenzofuran (DPBF)

Degradation of DPBF was studied under green LEDs illumination with 96 elements. The degradation was traced by measuring light absorbance at 430 nm after different illumination times. Fig. 5 shows results of initial blank tests with saturated solution containing nitrogen and oxygen only, as well as oxygen and nitrogen in the presence of nanocrystalline silicon. Concentration of DPBF does not change in the absence of PSi with either nitrogen or oxygen present in the system. In the presence of PSi, but no oxygen, a small decrease in concentration of DPBF was observed. This could be associated with incomplete substitution of oxygen after bubbling of nitrogen through solution, the presence of adsorbed oxygen in PSi, or with the adsorption of DPBF molecules onto the porous material having a reasonably high specific surface area.

The rate of DPBF concentration decrease was calculated using an equation similar to Eq. (2) with the measured rate of reaction, based on the samples taken from the liquid reservoir and substituting the measured number of photons. In the presence of silicon powder, but with no light the rate of decrease in DBPF, concentration was estimated to be 2.3×10^{-7} mol dm^{-3} s^{-1}. In the presence of oxygen and nanocrystalline silicon under green LEDs illumination the decrease in DBPF concentration is effectively linear and strongly depends on the oxygen flow rate. At a lower oxygen flow rate, the maximum rate of DPBF degradation is about 2.6×10^{-7} mol dm^{-3} s^{-1}, whereas at a higher flow rate, the corresponding reaction rate is about 1.2×10^{-6} mol dm^{-3} s^{-1}.

Conventionally, quantum yield of photochemical reactions is calculated in relation to the intensity of the incident light, measured by actinometry. However, in the case of singlet oxygen generation there are three additional steps which should be taken into consideration: (i) conversion of photons into excitons, (ii) conversion of excitons into singlet oxygen molecules, and (iii) efficiency of reaction of singlet oxygen with an organic substrate. Therefore, in this case quantum yield of chemical reaction can only be calculated as a ratio of the observed rate of reaction to the rate of singlet oxygen generation:

$$\Theta_R = \frac{r(\mathrm{DPBF})}{r(^1O_2)} = \frac{1.2 \times 10^{-6}\ \mathrm{mol\,dm^{-3}\,s^{-1}}}{3.5 \times 10^{-6}\ \mathrm{mol\,dm^{-3}\,s^{-1}}} = 34\% \qquad (3)$$

This value of quantum yield is calculated without making any assumptions on the intensity of incident light or geometry of the reactor, and thus reflects the true quantum efficiency of the reaction. The obtained value is quite high, which suggests that the proposed method of generation of singlet oxygen should give reasonable production yields in the reactions of synthetic interest.

4. Conclusions

Efficiency of electrical power to light of light emitting diodes and efficiency of light to absorbed photons of the developed LED based reactor were measured. The number of absorbed photons, measured by ferrioxalate actinometer, corresponded well with the power output of the light source, demonstrating high efficiency of the cylindrical laboratory photochemical reactor. This is likely due to the specific geometrical arrangement of the reactor, minimising absorbance of light by non-reflecting surfaces and having low scattering. Generation of singlet oxygen in the reactor system under irradiation by Ar^+ laser, green LEDs and UV LEDs was detected both by indirect measurement of suppression of photoluminescense of porous silicon, as well as directly by measuring luminescence due to relaxation of excited oxygen. These measurements were possible not only in CCl_4, but also in CH_2Cl_2 solvent which has considerably shorter lifetime of singlet oxygen. It is necessary to extend this work to more environmentally benign non-chlorinated solvents. The measured chemical reaction quantum yield, based on the decomposition of diphenylisobenzofuran, was about 34%. Therefore, this technology should find practical synthetic applications.

Acknowledgements

This work was funded by EPSRC via grants EP/D000564 and EP/E012183, the University of Bath's Enterprise Development Fund and in part by FP6 EC grant (STRP 013875).

References

[1] P. Esser, B. Pohlmann, H.-D. Scharf, The photochemical synthesis of fine chemicals with sunlight, Angew. Chem. Int. Ed. Engl. 33 (1994) 2009–2023.
[2] M.F.J. Dijkstra, H. Buwalda, A.W.F.d. Jong, A. Michorius, J.G.M. Winkelman, A.A.C.M. Beenackers, Experimental comparison of three reactor designs for photocatalytic water purification, Chem. Eng. Sci. 56 (2001) 547–555.
[3] R. Molinari, M. Mungari, E. Drioli, A.D. Paola, V. Loddo, L. Palmisano, M. Schiavello, Study of a photocatalytic membrane reactor for water purification, Catal. Today 55 (2000) 71–78.
[4] M.V. Twigg, Photocatalytic reactor. WO 03/035227, 2003.
[5] H.I.d. Lasa, J. Valladares, Photocatalytic reactor. US Patent 5,683,589 (1997).
[6] K. Hofstadlert, R. Bauer, S. Novallc, O. Heisler, New reactor design for photocatalytic wastewater treatment with TiO_2 immobilized on fused-silica glass fibers: photomineralization of 4-chlorophenol, Environ. Sci. Technol. 28 (1994) 670–674.
[7] Y.-S. Choi, B.-W. Kim, Photocatalytic disinfection of *E. coli* in a UV/TiO_2-immobilised optical–fibre reactor, J. Chem. Technol. Biotechnol. 75 (2000) 1145–1150.
[8] H.-S. Kim, M.-S. Kim, J.-H. Lee, S.-J. Yu, Photocatalytic LED purifier. WO0164318, 2001.
[9] H. Lin, K.T. Valsaraj, Development of an optical fiber monolith reactor for photocatalytic wastewater treatment, J. Appl. Electrochem. 35 (2005) 699–708.
[10] R. Gorges, S. Meyer, G. Kreisel, Photocatalysis in microreactors, J. Photochem. Photobiol. A: Chem. 167 (2004) 95–99.
[11] H. Lu, M.A. Schmidt, K.F. Jensen, Photochemical reactions and online UV detection in microfabricated reactors, Lab on a Chip 1 (2001) 22–28.
[12] G. Takei, T. Kitamori, H.-B. Kim, Photocatalytic redox-combined synthesis of L-pipecolinic acid with a titania-modified microchannel chip, Catal. Commun. 6 (2005) 357–360.
[13] Y. Matsushita, S. Kumada, K. Wakabayashi, K. Sakeda, T. Ichimura, Photocatalytic reduction in microreactors, Chem. Lett. 35 (2006) 410–411.
[14] S. Teekateerawej, J. Nishino, Y. Nosaka, Design and evaluation of photocatalytic micro-channel reactors using TiO_2-coated porous ceramics, J. Photochem. Photobiol. A: Chem. 179 (2006) 263–268.
[15] B.D.A. Hook, W. Dohle, P.R. Hirst, M. Pickworth, M.B. Berry, K.I. Booker-Milburn, A practical flow reactor for continuous organic photochemistry, J. Org. Chem. 70 (2005) 7558–7564.
[16] G. Carmignani, L. Frederick, S. Sitkiewitz, Apparatus and method for photocatalytic purification and disinfection of fluids. US Patent 6,902,653 (2005).
[17] D.H. Chen, X. Ye, K. Li, Oxidation of PCE with a UV LED photocatalytic reactor, Chem. Eng. Technol. 28 (2005) 95–97.
[18] C.G. Bochet, Wavelength-selective cleavage of photolabile protecting groups, Tetrahedron Lett. 41 (2000) 6341–6346.
[19] D. Kovalev, E. Gross, N. Künzner, F. Koch, V.Y. Timoshenko, M. Fujii, Resonant electronic energy transfer from excitons confined in silicon nanocrystals to oxygen molecules, Phys. Rev. Lett. 89 (2002) 137401.
[20] D. Kovalev, M. Fujii, Silicon nanocrystals: photosensitizers for oxygen molecules, Adv. Mater. 17 (2005) 2531–2544.
[21] M. Fujii, M. Usui, S. Hayashi, E. Gross, D. Kovalev, N. Künzner, J. Diener, V.Y. Timoshenko, Singlet oxygen formation by porous Si in solution., Phys. Stat. Sol. A 2002 (2005) 1385–1389.
[22] F. Wilkinson, W.P. Helman, A.B. Ross, Rate constants for the decay and reactions of the lowest electronically excited singlet state of molecular oxygen in solution. An expanded and revised compilation, J. Phys. Chem. Ref. Data 24 (1995) 663–1021.
[23] M. Fujii, M. Usui, S. Hayashi, E. Gross, D. Kovalev, N. Künzner, J. Diener, V.Y. Timoshenko, Chemical reaction mediated by excited states of Si nanocrystals—singlet oxygen formation in solution, J. Appl. Phys. 95 (2004) 3689–3693.
[24] E.A. Lissi, M.V. Encinas, E. Lemp, M.A. Rubio, Singlet oxygen O_2 ($^1\Delta_g$) bimolecular processes. Solvent and compartmentalization effects, Chem. Rev. 93 (1993) 699–723.
[25] C.G. Hatchard, C.A. Parker, A new sensitive chemical actinometer. II. Potassium ferrioxalate as a standard chemical actinometer, Proc. Roy. Soc. Lond. A 235 (1956) 518–536.
[26] J.F. Rabek, Experimental Methods in Photochemistry, Wiley, Chichester, 1982, p. 1098.
[27] J.M. Smith, Chemical Engineering Kinetics, 3rd ed., McGraw-Hill Book Company, 1981, p. 676.
[28] D. Kovalev, G. Polisski, M. Ben-Chorin, J. Diener, F. Koch, J. Appl. Phys. 80 (1996) 5978.
[29] T.A. Jenny, N.J. Turro, Solvent and deuterium effects on the lifetime of singlet oxygen determined by direct emission spectroscopy at 1.27 μm, Tetrahedron Lett. 23 (1982) 2923–2926.
[30] K.I. Salokhiddinov, I.M. Byteva, G.P. Gurinovich, Litetime of singlet oxygen in various solvents, J. Appl. Spectrosc. 34 (1981) 561–564.